Supplementary Data

Simulation and model description

Stochastic simulations were performed using MCell, version 3 [1,2] with a time step of 0.1 μs for calcium and 1.0 μs for all other molecules. The VDCC kinetics and PMCA pump kinetics used in the MCell and deterministic simulations are shown in Fig. S1 and S2, respectively. The deterministic simulations were performed using a cubic grid with a grid spacing of 25 nm and a time step of 0.25 μs. Furthermore, the kinetics of the reaction schemes shown in Fig. S1-4 were implemented by integrating the corresponding ODE. The calcium (C) and buffer (B_i^j) concentrations obey a simple diffusion equation:

$$\frac{\partial C}{\partial t} = D_{Ca}\nabla^2 C + \sum G_{bind}(C, B_i^{\,j})$$

$$\frac{\partial B_i^{\,j}}{\partial t} = D_B \nabla^2 B_i^{\,j} + H(C, B_i^{\,j})$$

where B_i^j represent the different states of the buffer as shown in the reaction diagram of Fig. S3. The last terms in these diffusion equations, G_{bind} and H, represent to a straightforward incorporation of the calcium-buffer binding reactions. For example, the term involving $B_1^{\,0}$ in the equation for C reads $B_1^{\,0}$ [$-2k^+C - k_+C + k_-$] since $B_1^{\,0}$ can bind calcium to transition to $B_2^{\,0}$ and $B_1^{\,1}$ and can unbind calcium to transition to $B_0^{\,0}$. Similarly, the term in the equation for $B_1^{\,0}$ can be found by counting all arrows starting from or ending at $B_1^{\,0}$ and reads:

$$-B_1^{\,0}[2k^+C + k_+C + k_-] + 2k_+C\,B_0^{\,0} + 2k_-B_2^{\,0} + k^-B_1^{\,1}.$$

These equations are implemented with the relevant boundary conditions at the faces of the simulation box. Finally, the kinetic scheme for the two models of the calcium sensor is shown in Fig. S4. In these schemes, F represents the fused (released) vesicle while V

represents the fraction of vesicles that can be released. At the start of a simulation the latter is set to 1 while the different states of the sensor are determined as the equilibrium values corresponding to a resting calcium concentration of 100 nM. The equations for the sensor dynamics are solved either deterministically or stochastically, using a time step of 0.1 μs. The sensor had a size of 66 nm^2 in the MCell simulations. All rates and further relevant parameters are given in Table 1.

The role of depletion

The effect of ligand depletion can be investigated in a simple radially symmetric model in which a single sensor of size R_0 binds ions at a rate k_{on}. After binding, the ligand is removed permanently and the sensor is immediately able to rebind an ion. To obtain a non-trivial steady state solution we furthermore assume that the concentration at a distance larger than R_0 ($r=R_1$) is fixed at C_∞. Within the computational box the ion concentration obeys the simple diffusion equation with as boundary condition at $r=R_0$: $DA\left.\frac{\partial C}{\partial r}\right|_{R_0} = k_{on}C(R_0)$ where $A = 4\pi R_0^2$ is the surface area of the receptor. Then, we can find the steady state solution for this problem as:

$$C(r) = C_\infty - \frac{k_{on}C_\infty}{2\pi D + k_{on}(\frac{1}{R_0} - \frac{1}{R_1})}(\frac{1}{R_0} - \frac{1}{R_1})$$

At the sensor site and for $R_0 << R_1$ we find $C(R_0) \approx \frac{C_\infty}{1 + \frac{k_{on}}{2\pi D R_0}}$

giving us a binding rate of $k_{on}C(R_0)$. Thus, the deviation of the local sensor concentration from the imposed concentration is controlled by the parameter combination $\frac{k_{on}}{2\pi D R_0}$: a smaller sensor size, a smaller diffusion constant or a larger on rate increases the depletion

effect. Clearly, as long as $\frac{k_{on}}{2\pi DR_0} << 1$ we can safely neglect the effects of local depletion. A similar conclusion was reached numerically by Hake and Lines [3].

It is important to note that the removal of calcium ions by a sensor can be incorporated in a deterministic model. To this end, we include the binding of ligands as an effective flux term, only present as a boundary condition for the ligand concentration at the voxel that contains the sensor. This flux term is written as $DA\nabla C = k_{on}C$ where A is the area of the voxel face. Through explicit simulations, we have verified that for this simplified model the deterministic approach gives the same steady state solution as a full stochastic calculation using MCell.

We have also implemented local calcium ion removal into the deterministic simulation for our model synapse. The sensor was placed at 250 nm of the VDCC cluster and had a size equal to the grid size (25 nm). In Fig. S5 we plot the percentage difference between the deterministic calculation with and without local depletion as a function of the release probability. For our parameter values, this difference is at most 7%.

Table 1 Model parameters

Parameter	**Value**
Calcium diffusion constant (D_{Ca}) [4]	220 $\mu m^2/s$
Calbindin diffusion constant (D_B) [5]	28 $\mu m^2/s$
Resting intracellular calcium concentration	100 nM
Intracellular calbindin concentration [6]	45 μM

PMCA surface density [7]	180 / μm^2
VDCC number [8]	1 - 208
Distance between the sensor and the VDCC cluster [9]	10 – 400 nm
Maximum radius of the VDCC cluster	66 nm
Calbindin [10]	
Association rate, high affinity site (k^+)	0.55×10^7 /M s
Dissociation rate, high affinity site (k^-)	2.6 /s
Association rate, medium affinity (k_+)	4.35×10^7 /M s
Disassociation rate, medium affinity (k_-)	35.8 /s
PMCA [7]	
Association rate (k_{p01})	1.5×10^7 /M s
Association rate (k_{p10})	20 /s
Transition rate 1 (k_{12})	20 /s
Transition rate 2 (k_{23})	100 /s
Leak rate (k_{leak})	12.5 /s
VDCC	

Dynamics [11]	$a_i(v) = a_{i0} \exp(v/v_i)$ and $b_i(v) = b_{i0}\exp(-v/v_i)$
$a_{10}, a_{20}, a_{30}, a_{40}$	4.04, 6.70, 4.39, 17.33 /ms
$b_{10}, b_{20}, b_{30}, b_{40}$	2.88, 6.30, 8.16, 1.84 /ms
v_1, v_2, v_3, v_4	49.14, 42.08, 55.31, 26.55 mV
Calcium sensor model [12]	
α	0.3 /μM ms
β	3 /ms
γ	30 /ms
δ	8 /ms
ρ	40 /ms

FIGURES

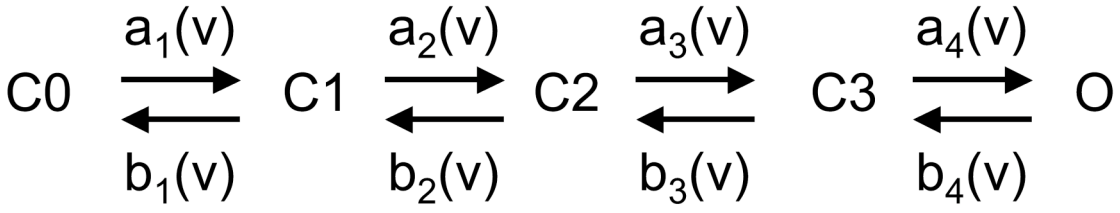

Fig. S1 Reaction scheme for the voltage dependent calcium channels, with O representing the open state. The dependence of the rates on the voltage can be found in Table 1.

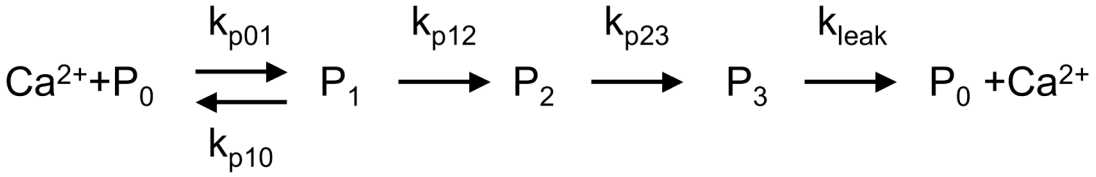

Fig. S2 Reaction scheme of the binding of PMCA pumps (rates given in Table 1).

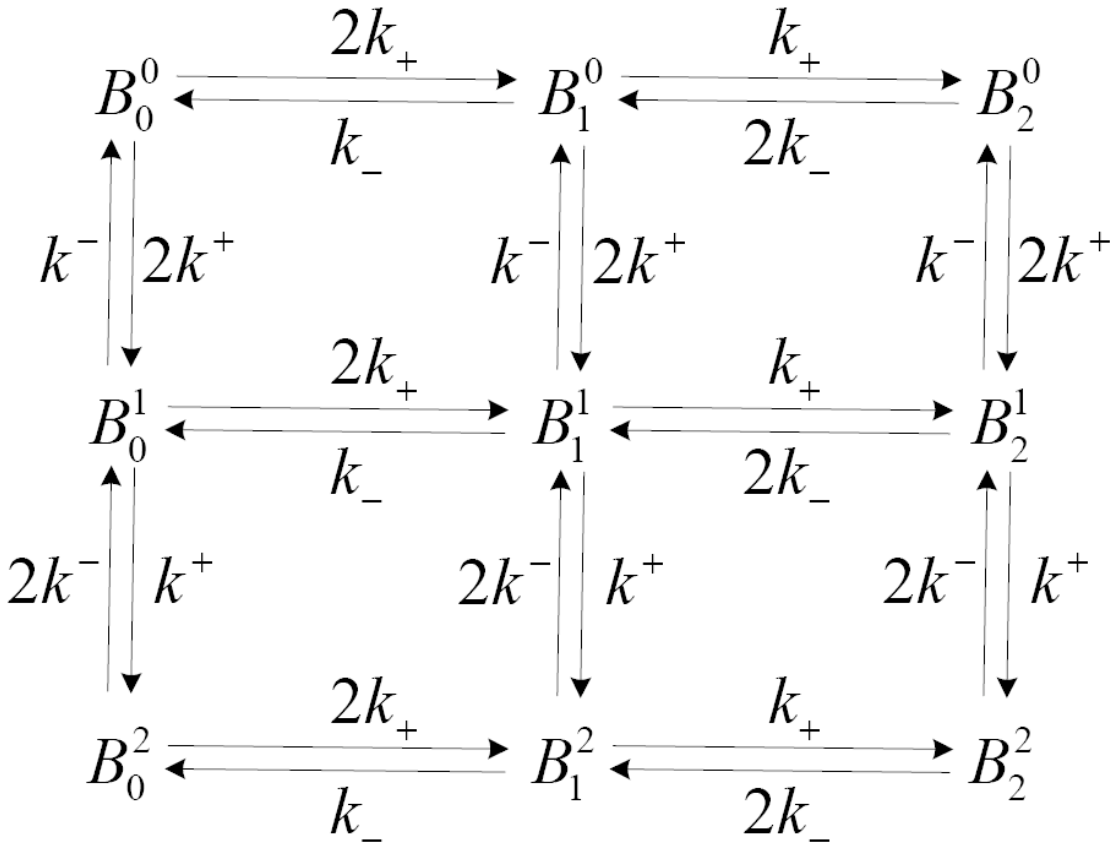

Fig. S3 Reaction scheme of the binding of calcium to the buffer calbindin. Each buffer molecule can bind up to 4 calcium ions and the rates for the reactions can be found in Table 1.

Model A

$$X \underset{\beta}{\overset{5\alpha[\mathrm{Ca}^{2+}]}{\rightleftarrows}} XCa_1 \underset{2\beta}{\overset{4\alpha[\mathrm{Ca}^{2+}]}{\rightleftarrows}} XCa_2 \underset{3\beta}{\overset{3\alpha[\mathrm{Ca}^{2+}]}{\rightleftarrows}}$$

$$XCa_3 \underset{4\beta}{\overset{2\alpha[\mathrm{Ca}^{2+}]}{\rightleftarrows}} XCa_4 \underset{5\beta}{\overset{\alpha[\mathrm{Ca}^{2+}]}{\rightleftarrows}} XCa_5 \underset{\delta}{\overset{\gamma}{\rightleftarrows}} XCa_5^* \xrightarrow{\rho} F$$

Model B

$$X \underset{\beta}{\overset{5\alpha[\mathrm{Ca}^{2+}]}{\rightleftarrows}} XCa_1 \underset{2\beta}{\overset{4\alpha[\mathrm{Ca}^{2+}]}{\rightleftarrows}} XCa_2 \underset{3\beta}{\overset{3\alpha[\mathrm{Ca}^{2+}]}{\rightleftarrows}}$$

$$XCa_3 \underset{4\beta}{\overset{2\alpha[\mathrm{Ca}^{2+}]}{\rightleftarrows}} XCa_4 \underset{5\beta}{\overset{\alpha[\mathrm{Ca}^{2+}]}{\rightleftarrows}} XCa_5 \underset{\delta}{\overset{\gamma}{\rightleftarrows}} XCa_5^*$$

$$V \xrightarrow{\rho XCa_5^*} F$$

Fig. S4 Kinetic description of the two release models used in the paper. Model A correspond to a sensor that controls a single vesicle. This one-to-one correspondence is relaxed in model B where V is the fraction of the vesicles that are capable of being released.

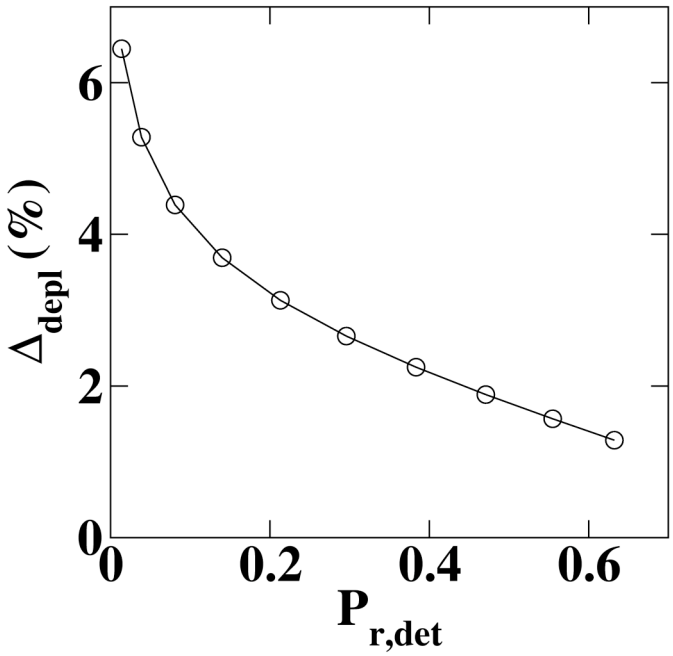

Fig. S5 Difference between the release probability in a deterministic calculation with and without local removal of calcium ions as a function of the release probability. The distance between the cluster and the sensor was taken to be 250 nm. The solid line is a guide to the eye.

1. Stiles, J. R., D. Van Helden, T. M. Bartol, E. E. Salpeter, and M. M. Salpeter. Miniature endplate current rise times less than 100 microseconds from improved dual recordings can be modeled with passive acetylcholine diffusion from a synaptic vesicle. *PNAS* **93**:5747-5752 (1996).
2. Kerr, R. A., T. M. Bartol, B. Kaminsky, M. Dittrich, J.-C. J. Chang, S. B. Baden, T. J. Sejnowski and J. R. Stiles 2008. Fast Monte Carlo simulation methods for biological reaction-diffusion systems in solution and on surfaces. *SIAM J. Sci. Comput.* **30**: 3126 (2008).
3. Hake, J. and G. T. Lines. Stochastic binding of Ca2+ ions in the dyadic cleft; continuous versus random walk description of diffusion. *Biophys J* **94**: 4184-4201 (2008).
4. Allbritton, N., T. Stryer, and L. Stryer. Range of Messenger Action of Calcium Ion and Inositol 1,4,5-Trisphosphate. *Science* **258**:1812-1815 (1992).
5. Schmidt, H., K. M. Stiefel, P. Racay, B. Schwaller, and J. Eilers. Mutational

analysis of dendritic Ca2+ kinetics in rodent Purkinje cells: role of parvalbumin and calbindin D28k. *J Physiol (Lond)* **551**:13-32 (2003).
6. Müller, A., M. Kukley, P. Stausberg, H. Beck, W. Müller, and D. Dietrich. Endogenous Ca2+ buffer concentration and Ca2+ microdomains in hippocampal neurons. *J Neurosci* **25**:558-565 (2005).
7. Sneyd, J., K. Tsaneva-Atanasova, J. I. Bruce, S. V. Straub, D. R. Giovannucci, and D. I. Yule. 2003. A model of calcium waves in pancreatic and parotid acinar cells. *Biophys J* **85**:1392-1405 (2003).
8. Koester, H. J., and B. Sakmann. Calcium dynamics associated with action potentials in single nerve terminals of pyramidal cells in layer 2/3 of the young rat neocortex. *J Physiol (Lond)* **529** Pt 3:625-646 (2000).
9. Meinrenken, C. J., J. G. Borst, and B. Sakmann. Calcium secretion coupling at calyx of held governed by nonuniform channel-vesicle topography. *J Neurosci* **22**:1648-1667 (2002).
10. Nägerl, U. V., D. Novo, I. Mody, and J. L. Vergara. Binding kinetics of calbindin-D(28k) determined by flash photolysis of caged Ca(2+). *Biophys J* **79**:3009-3018 (2000).
11. Bischofberger, J., J. R. Geiger, and P. Jonas. Timing and efficacy of Ca2+ channel activation in hippocampal mossy fiber boutons. *J Neurosci* **22**:10593-10602 (2002).
12. Bollmann, J. H., B. Sakmann, and J. G. Borst. Calcium sensitivity of glutamate release in a calyx-type terminal. *Science* **289**:953-957 (2000).